

O^&d[] &U~]]|^ { ^} æ^ T æ! æ ç UØ- | O@{ O[{ { E
V@ ð } !} æ ã î V@ Û[^ æ U[& ã ç [~ Ö @ { ã d ^ GFI

Electronic Supplementary Information

Ultrahigh volatile iodine uptake by hollow microspheres formed from a heteropore covalent organic framework

Zhi-Jian Yin,^{a,b} Shun-Qi Xu,^a Tian-Guang Zhan,^a Qiao-Yan Qi,^a Zong-Quan Wu^b
and Xin Zhao*^a

^a CAS Key Laboratory of Synthetic and Self-assembly Chemistry for Organic Functional Molecules, Shanghai Institute of Organic Chemistry, Chinese Academy of Sciences, 345 Lingling Road, Shanghai 200032, China

^b Department of Polymer Science and Engineering, School of Chemistry and Chemical Engineering, Anhui Key Laboratory of Advanced Functional Materials and Devices, Hefei University of Technology, Anhui Province, Hefei 230009, China

Email: xzhao@sioc.ac.cn.

Table of Contents

Section 1. Instruments and Methods	3-5
Section 2. Synthesis and Characterizations	5-8
Figure S1. TGA profile of SIOC-COF-7	8
Figure S2. FT-IR spectra of monomers and SIOC-COF-7	9
Figure S3. BET surface area plot	9
Figure S4. Illustration for pore size distribution	10
Figure S5. TGA profile of iodine-loaded SIOC-COF-7	10
Figure S6. TEM images of SIOC-COF-7 and iodine-loaded SIOC-COF-7	11
Figure S7. Diagram of recyclability for iodine uptake	11
Figure S8. Photographs of iodine capture in solution phase	12
Figure S9. Working curve for the estimation of iodine uptake in solution	12
Figure S10. Photographs of iodine release in solution phase	12
Table S1. Summary of iodine uptake properties of porous materials	13
References for Table S1	13-15
Table S2. Fractional atomic coordinates	15-19
Figure S9-S12. ¹H NMR and ¹³C NMR spectra of new compounds	20-21

Section 1. Instruments and Methods

Fourier transform infrared spectroscopy (FTIR)

Fourier transform infrared spectroscopy (FTIR) was carried out with a Nicolet 380 FTIR spectrometer. The samples for IR study were prepared as KBr pellets.

Thermal gravimetric analysis (TGA)

Thermal gravimetric analyses were carried out on a Waters TGA Q500 by heating the samples from 25 to 950 or 1000 °C under nitrogen atmosphere at a heating rate of 10 °C/min.

UV-vis absorption spectra (UV-vis)

UV-vis experiments were performed on a Unico 4802 UV-vis double beam spectrophotometer.

Transmission electron microscopy (TEM) and Energy dispersive X-ray spectroscopy (EDX)

Transmission electron microscopy and Energy dispersive X-ray spectroscopy (EDX) were performed on a Tecnai G2 F20 S-TWIN or a GEOL JEM-2100 instrument.

Powder X-ray diffraction (PXRD)

Powder X-ray diffraction measurement was carried out with an X'Pert PROX system using monochromated Cu/K α ($\lambda = 0.1542$ nm). The sample was spread on the square recess of XRD sample holder as a thin layer.

Nitrogen adsorption-desorption isotherm measurements

The measurements were carried out using a Quadrasorb SI MP. Before gas adsorption measurements, the as-prepared sample (~50 mg) was activated by being immersed in anhydrous 1,4-dioxane for 12 h. The solvent was decanted and the sample was dried under dynamic vacuum at 160 °C for 4 h. The resulting sample was then used for gas

adsorption measurements from 0 to 1 atm at 77 K. The Brunauer-Emmett-Teller (BET) method was utilized to calculate the specific surface area. By using the non-local density functional theory model, the pore size distribution curve was derived from the sorption data.

Structural simulations and powder X-ray diffraction analysis

The Pawley refinement of the experimental PXRD was conducted by the Reflux module in the Materials Studio 7.0. Before the simulations, the structure was firstly optimized in Gaussian 09 package by semiempirical calculations at PM3 level. The simulation of the two possible structures was carried out in Accelrys Materials Studio 7.0 software package. The stimulated PXRD patterns were determined by the Reflex module. P1 space group was used for the simulations.

Experiment procedure for the uptake of iodine vapor

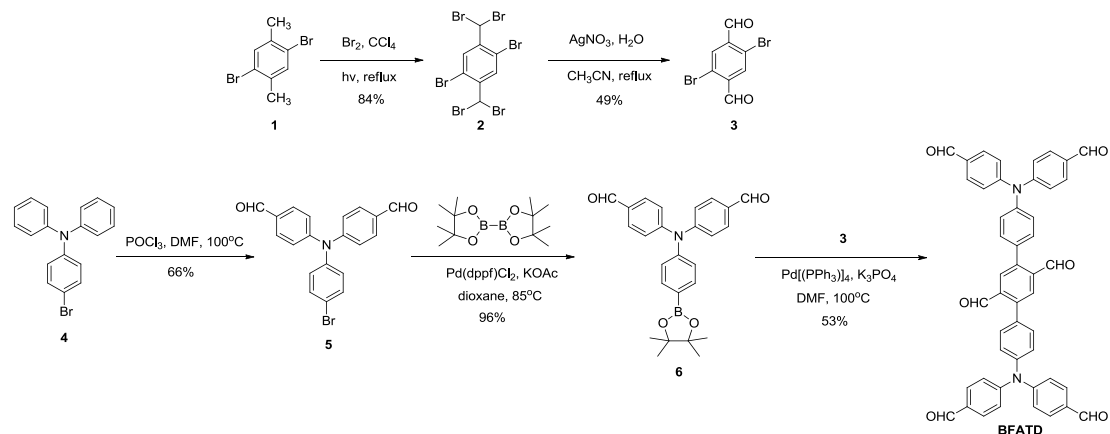
The iodine capture experiment was performed in the following procedure. Activated **SIOC-COF-7** (43.6 mg) in a small beaker and excess iodine were placed in a sealed glass container, heated at 75 °C under ambient pressure. Some contact time later, the COF sample was cooled down to room temperature and weighed. The iodine uptake of **SIOC-COF-7** was calculated by weight gain: $\alpha = [(m_2 - m_1)/m_1] \times 100 \text{ wt } \%$, where α is the iodine uptake, m_1 and m_2 are the mass of **SIOC-COF-7** sample before and after being exposed to iodine vapor, respectively. The iodine capture experiments were conducted three times and a good repeatability was observed.

Experiment procedure for the uptake of iodine in solution phase

The iodine capture experiment in solution phase was performed in the following procedure. Iodine (40.0 mg) was dissolved in n-hexane (3.0 mL) and then activated **SIOC-COF-7** (30.0 mg) was added. Four days later, UV-vis absorption of the solution was recorded. The amount of iodine remained in solution was determined by

using the working curve established (Figure S10). Then the amount of iodine captured by the COF can be calculated through subtracting the amount of iodine remained in solution from the initial amount of iodine.

Section 2. Synthesis and Characterizations



1,4-dibromo-2,5-bis(dibromomethyl)benzene (2) was synthesized following a reported procedure^[1] with minor modifications as detailed below. To a refluxing solution of 1,4-dibromo-2,5-dimethylbenzene (1.3 g, 5.0 mmol) in carbon tetrachloride (100 mL), which was irradiated with a 500 W incandescent lamp, a solution of bromine (1.3 mL, 25.3 mmol) in carbon tetrachloride (5 mL) was added dropwise. The reaction mixture was stirred under reflux with concomitant irradiation by the same lamp for 12 h. After being cooled to room temperature, the reaction mixture was washed successively with an aqueous solution of Na₂SO₃ and water, dried over anhydrous MgSO₄, and concentrated under reduced pressure. Recrystallization of the crude product from ethyl acetate yielded compound **2** as white crystals (2.4 g, 84%). ¹H NMR (400 MHz, CDCl₃): δ 8.13 (s, 2 H), 6.93 (s, 2H).

2,5-dibromoterephthalaldehyde (3) was synthesized following a reported procedure^[1] with minor modifications as detailed below. A solution of AgNO₃ (1.3 g, 7.7 mmol) in water (3.5 mL) was added to a suspension of 1,4-dibromo-2,5-bis(dibromomethyl)benzene (1.0 g, 1.7 mmol) in acetonitrile (24 mL) and the resulting mixture was stirred and heated to reflux under an argon atmosphere

for about 8 h. The reaction mixture was filtered while hot, and the solid was washed with hot acetonitrile. The filtrate was cooled to room temperature to allow crystallization of the product. The resulting needle-like crystals were collected by filtration, and the filtrate was concentrated to allow crystallization again. The combined crystals were dissolved in dichloromethane and the insoluble fraction was filtered off. The solvent was evaporated to yield compound **3** (0.25 g, 49%). ¹H NMR (400 MHz, CDCl₃): δ 10.35 (s, 2H), 8.16 (s, 2H).

4,4'-((4-bromophenyl)azanediyl)dibenzaldehyde (5) was synthesized following a reported procedure^[2] with minor modifications as detailed below. 4-bromo-N,N-diphenylaniline (6.0 g, 18.5 mmol) was dissolved in DMF (23 mL, 296 mmol) in a 250 mL flask. Under cooling with ice phosphorus oxychloride was added (18.5 mL, 198 mmol) dropwise. The solution was heated for 36 h at 100 °C. Upon being cooled to room temperature, the reaction was quenched by pouring it into ice-cold water. The reaction solution was neutralized with 2N NaOH solution, whereby a brown solid precipitated out. The solid was filtered, washed with water and ethanol. The crude product was purified by flash column chromatograph (dichloromethane/hexane 3:1) to give compound **5** as a yellow solid (4.64 g, 66%). ¹H NMR (400 MHz, CDCl₃): δ 9.91 (s, 2H), 7.79 (d, *J* = 8.6 Hz, 4H), 7.50 (d, *J* = 8.7 Hz, 2H), 7.18 (d, *J* = 8.6 Hz, 4H), 7.05 (d, *J* = 8.7 Hz, 2H).

4,4'-((4-(4,4,5,5-tetramethyl-1,3,2-dioxaborolan-2-yl)phenyl)azanediyl)dibenzaldehyde (6). Compound **5** (5.0 g, 13.1 mmol), bis(pinacolato)diborane (4.0 g, 15.8 mmol), potassium acetate (3.9 g, 39.7 mmol), Pd(dppf)₂Cl₂ (0.3 g, 0.4 mmol), and dried 1,4-dioxane (90 mL) were added in a 250 mL flask. The mixture was degassed through three freeze–pump–thaw cycles under an argon atmosphere and then stirred at 100 °C for 24 h. After being cooled to room temperature, the reaction mixture was extracted with ethyl acetate and dried over MgSO₄. After removed of solvent under reduced pressure, the crude product was purified by flash column chromatograph

(petroleum ether/ethyl acetate 10:1) to give compound **6** as a light yellow solid (5.4 g, 96%). ¹H NMR (400 MHz, CDCl₃): δ 9.90 (s, 2H), 7.81 (d, *J* = 8.4 Hz, 2H), 7.78 (d, *J* = 8.7 Hz, 4H), 7.19 (d, *J* = 8.6 Hz, 4H), 7.15 (d, *J* = 8.4 Hz, 2H), 1.46-1.27 (m, 12H). ¹³C NMR (125 MHz, CDCl₃): δ 190.50, 151.81, 148.18, 136.56, 131.59, 131.30, 125.55, 123.27, 84.01, 24.88. MS (ESI): *m/z* 428.4 [M+H]⁺. HRMS (ESI): Calcd for C₂₆H₂₇BNO₄ [M+H]⁺: 427.2064. Found: 427.2064.

4,4''-bis(bis(4-formylphenyl)amino)-[1,1':4',1''-terphenyl]-2',5'-dicarbaldehyde (BFTDA). A mixture of compound **3** (200 mg, 0.69 mmol), compound **6** (586 mg, 1.37 mmol), K₃PO₄ (182 mg, 0.86 mmol) and Pd[P(Ph₃)₄] (81 mg, 0.07 mmol) was dissolved in DMF (10 mL) in a 25 mL flask. The mixture was degassed through three freeze–pump–thaw cycles under an argon atmosphere and then stirred at 100 °C for 24 hours. After being cooled to room temperature, the reaction mixture was extracted with dichloromethane. The organic layer was washed with water, dried over MgSO₄, filtered and evaporated. The crude product was purified by flash column chromatograph (dichloromethane/ethyl acetate 50:1) to give **BFTDA** as a bright yellow solid (532 mg, 53%). ¹H NMR (500 MHz, DMSO-*d*₆): δ 10.11 (s, 2H), 9.91 (s, 4H), 8.02 (s, 2H), 7.89 (d, *J* = 8.6 Hz, 8H), 7.62 (d, *J* = 8.4 Hz, 4H), 7.35 (d, *J* = 8.4 Hz, 4H), 7.29 (d, *J* = 8.6 Hz, 8H). ¹³C NMR (125 MHz, CDCl₃): δ 191.28, 190.47, 151.66, 146.34, 143.56, 136.49, 133.43, 131.94, 131.64, 131.48, 130.49, 126.27, 123.52. MS (MALDI-TOF): *m/z* 732.2. HRMS (MALDI-TOF): Calcd for C₄₈H₃₂N₂O₆: 732.2251. Found: 732.2255.

Preparation of SIOC-COF-7. A mixture of BFATD (30 mg, 0.04 mmol), 1,4-diaminobenzene (13.3 mg, 0.12 mmol), 1,4-dioxane (0.5 mL), 1,3,5-trimethylbenzene (0.5 mL) and acetic acid (6 M (aq.), 0.1 mL) was placed in a glass ampoule. The mixture was sonicated for 3 minutes and then degassed through three freeze–pump–thaw cycles. After that the tube was sealed under vacuum and then warmed to room temperature. The mixture was heated to 120 °C for 3 days without

disturbance. After being cooled to room temperature, the solvent was evaporated, the yellow residue was washed with large amount of 1,4-dioxane and dichloromethane, and dried under vacuum to yield the COF (31.4 mg, 80.8%). Anal. Calcd. For $C_{66}H_{44}N_8$: C, 83.52; H, 4.67; N, 11.81. Found: C, 80.00; H, 4.78; N, 10.99.

References for the synthesis

(1) G. K. Paul, J. Mwaura, A. A. Argun, P. Taranekar and J. R. Reynolds, *Macromolecules*, 2006, **39**, 7789–7792.

(2) X. Yang, D. Liu and Q. Miao, *Angew. Chem.Int. Ed.*, 2014, **53**, 6786–6790.

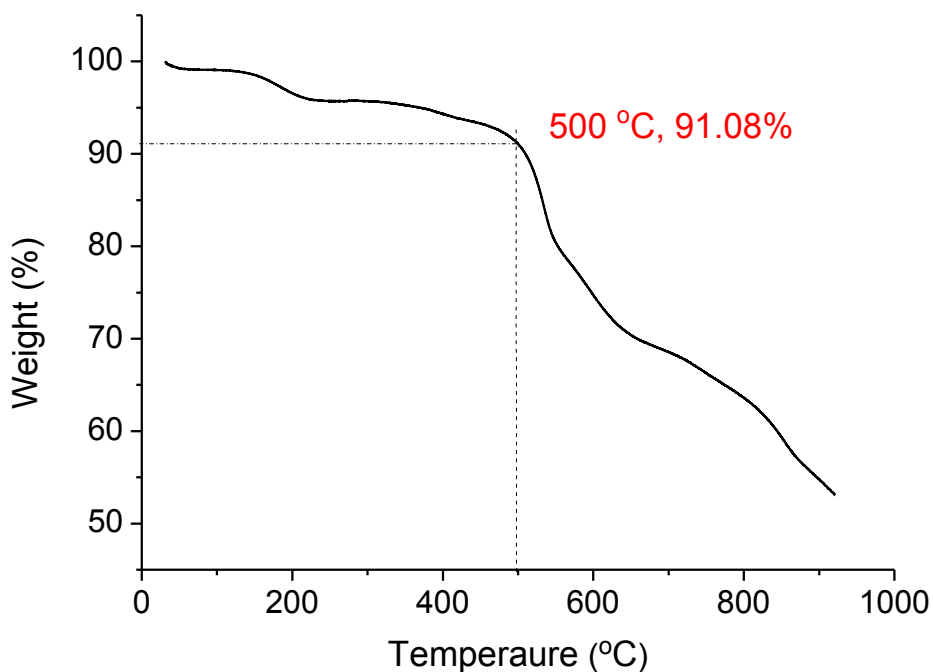


Fig. S1 TGA profile of **SIOC-COF-7**.

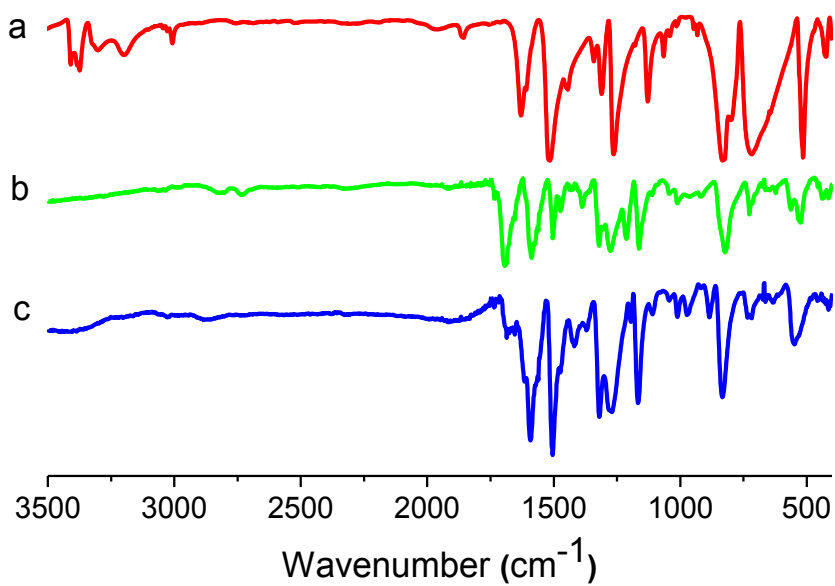


Fig. S2 FTIR spectra of (a) 1,4-diaminobenzene, (b) BFATD, and (c) **SIOC-COF-7**.

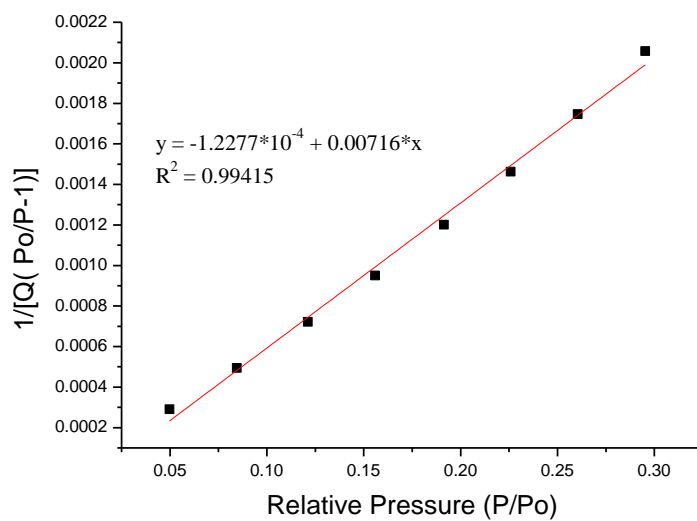


Fig. S3 BET surface area plot for **SIOC-COF-7** calculated from the isotherm.

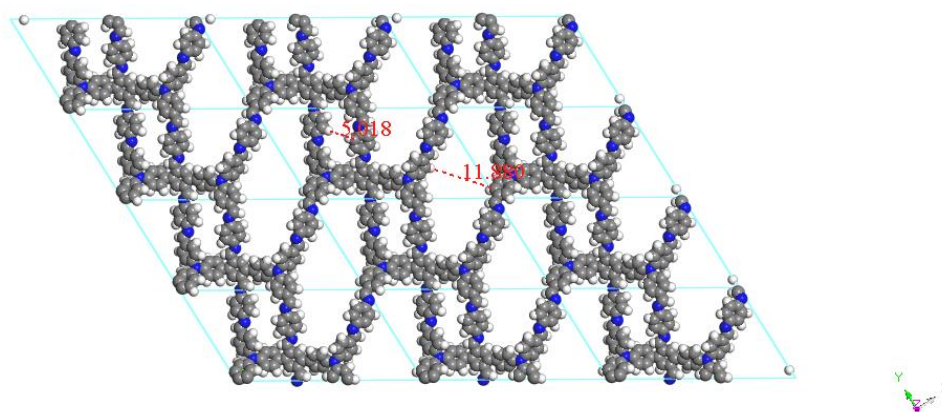


Fig. S4 Illustration for pore size distribution of **SIOC-COF-7** with eclipsed AA stacking.

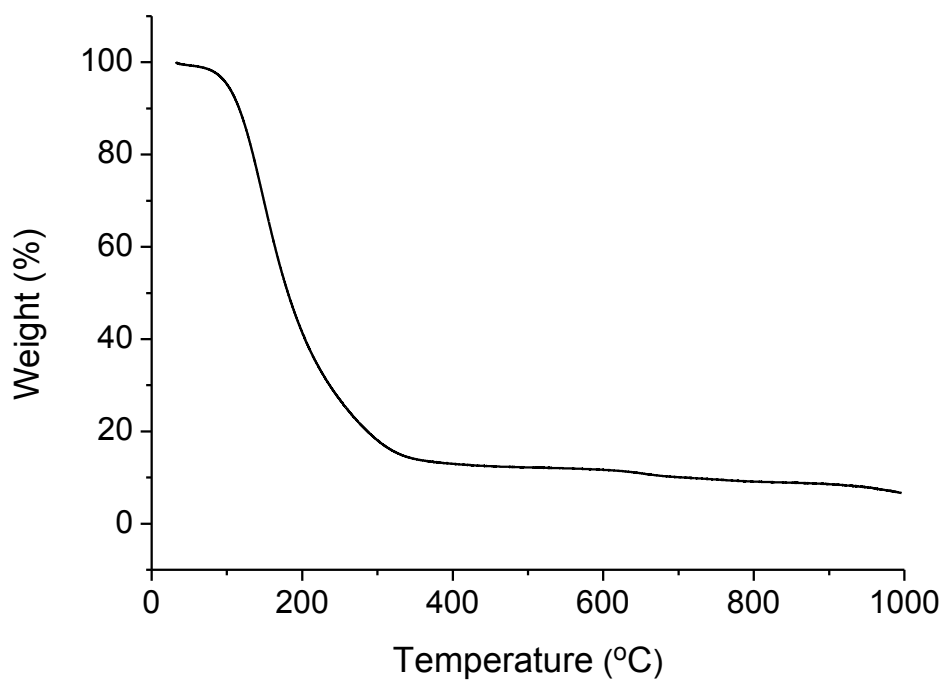


Fig. S5 TGA profile of iodine-loaded **SIOC-COF-7**.

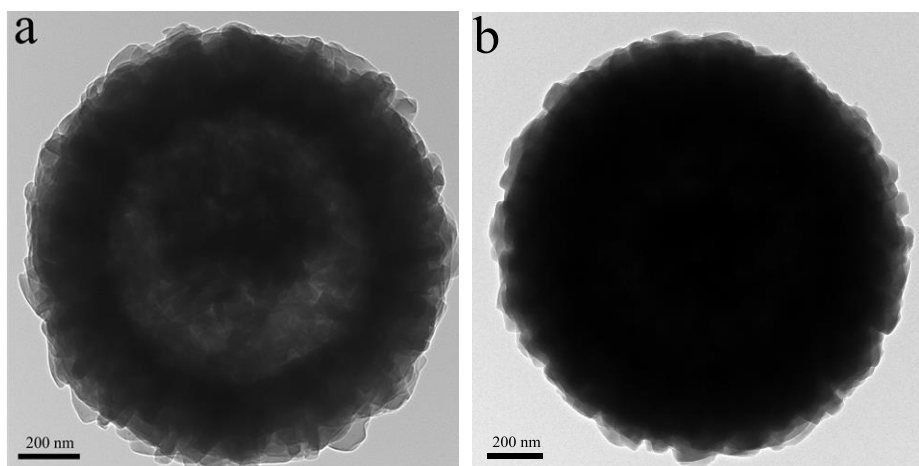


Fig. S6 TEM images of (a) **SIOC-COF-7** and (b) iodine-loaded **SIOC-COF-7**.

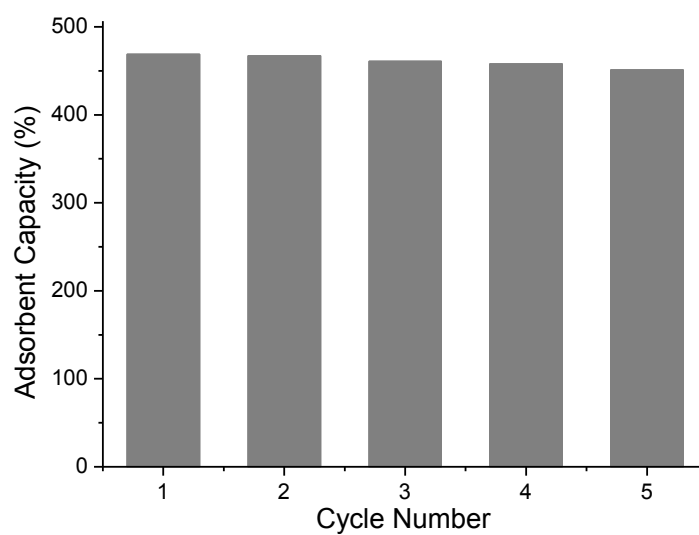


Fig. S7 Reusability of **SIOC-COF-7** for iodine capture. A sample with initial iodine uptake of 469 wt % was used for the recycle test.

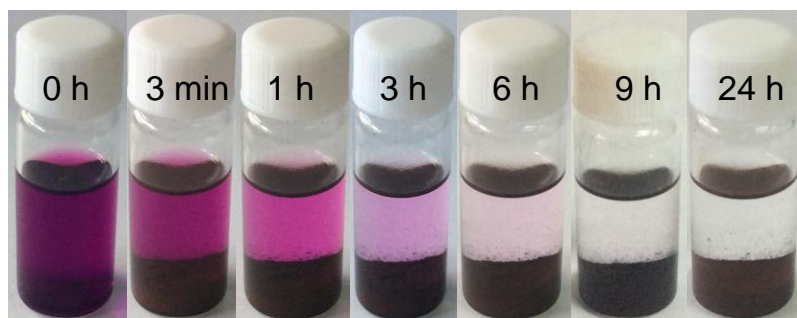


Fig. S8 Photographs showing progress of iodine capture after **SIOC-COF-7** (30 mg) was immersed in a hexane solution of iodine (10.0 mmol L^{-1} , 3 mL).

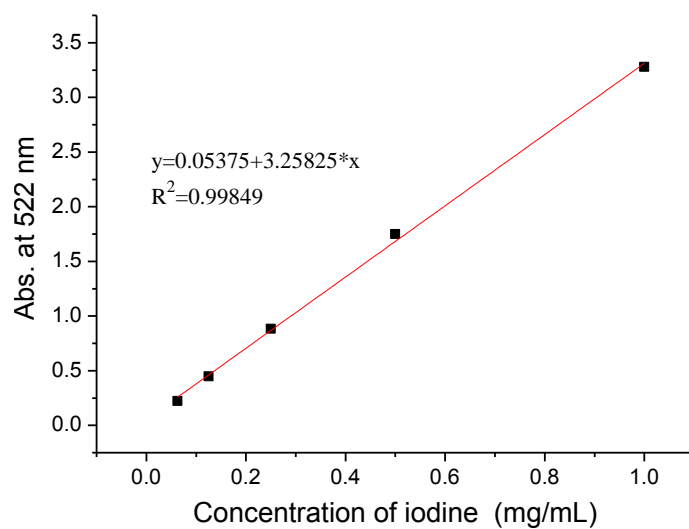


Fig. S9 Working curve for the estimation of iodine uptake in solution.

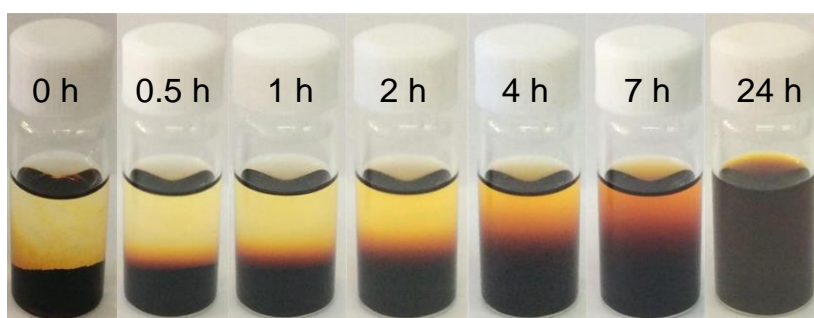


Fig. S10 Photographs showing progress of iodine release from the iodine-loaded **SIOC-COF-7** after it was immersed in ethanol.

Table S1. Summary of iodine uptake properties of porous materials.

Adsorbent	Temperature (°C)	pressure	S_{BET} (m ² g ⁻¹)	Iodine capacity (mg I ₂ /g)	References
1 SIOC-COF-7	75	1 bar	618	4810	This work
2 HCMP-3(reduced)	85	1 bar	82	3360	S1
3 AzoPPN	77	1 bar	400	2900	S2
4 PAF-24	75	1 bar	136	2760	S3
5 PAF-23	75	1 bar	82	2710	S3
6 PAF-25	75	1 bar	262	2600	S3
7 Azo-Trip	77	1 bar	510	2380	S4
8 NiMoS chalcogels	60	1 bar	490	2250	S5
9 CMPN-3	70	1 bar	1368	2080	S6
10 NiP-CMP	77	1 bar	2630	2020	S7
11 PAF-1	25	40 Pa	5600	1860	S8
12 NTP	75	1 bar	1067	1800	S9
13 JUC-Z2	25	40 Pa	2081	1440	S8
14 Cu-BTC	75	1 bar	–	1750	S10
15 ZIF-8	75	1 bar	1875	1200	S11
16 Activated carbon	75	1 bar	–	300	S9
17 Ag@Zeolite	95	1 bar	–	275	S12
Mordenites					
18 Ag@Mon-POF	70	1 bar	690	250	S13
19 CC3	20	1 bar	–	364	S14

References for Table S1

(S1) Y. Liao, J. Weber, B. M. Mills, Z. Ren and C. F. J. Faul, Highly efficient and reversible iodine capture in hexaphenylbenzene-based conjugated microporous polymers. *Macromolecules*, 2016, **49**, 6322–6333.

- (S2) H. Li, X. Ding and B.-H. Han, Porous azo-bridged porphyrin-phthalocyanine network with high iodine capture capability. *Chem. Eur. J.*, 2016, **22**, 11863 – 11868.
- (S3) Z. Yan, Y. Yuan, Y. Tian, D. Zhang and G. Zhu, Highly efficient enrichment of volatile iodine by charged porous aromatic frameworks with three sorption sites. *Angew. Chem. Int. Ed.*, 2015, **54**, 12733–12737.
- (S4) Q.-Q. Dang, X.-M. Wang, Y.-F. Zhan and X.-M. Zhang, An azo-linked porous triptycene network as an absorbent for CO₂ and iodine uptake. *Polym. Chem.*, 2016, **7**, 643–647.
- (S5) K. S. Subrahmanyam, D. Sarma, C. D. Malliakas, K. Polychronopoulou, B. J. Riley, D. A. Pierce, J. Chun and M. G. Kanatzidis, Chalcogenide aerogels as sorbents for radioactive iodine. *Chem. Mater.*, 2015, **27**, 2619-2626.
- (S6) Y. Chen, H. Sun, R. Yang, T. Wang, C. Pei, Z. Xiang, Z. Zhu, W. Liang, A. Li, and W. Deng, Synthesis of conjugated microporous polymer nanotubes with large surface areas as absorbents for iodine and CO₂ uptake. *J. Mater. Chem. A*, 2015, **3**, 87-91.
- (S7) S. A. Y. Zhang, Z. Li, H. Xia, M. Xue, X. Liu and Y. Mu, Highly efficient and reversible iodine capture using a metalloporphyrin-based conjugated microporous polymer. *Chem. Commun.*, 2014, **50**, 8495–8498.
- (S8) C. Pei, T. Ben, S. Xu and S. Qiu, Ultrahigh iodine adsorption in porous organic frameworks. *J. Mater. Chem. A*, 2014, **2**, 7179–7187.
- (S9) H. Ma, J.-J. Chen, L. Tan, J.-H. Bu, Y. Zhu, B. Tan and C. Zhang, Nitrogen-rich triptycene-based porous polymer for gas storage and iodine enrichment. *ACS Macro Lett.*, 2016, **5**, 1039–1043.
- (S10) D. F. Sava, K. W. Chapman, M. A. Rodriguez, J. A. Greathouse, P. S. Crozier, H. Zhao, P. J. Chupas and T. M. Nenoff, Competitive I₂ sorption by Cu-BTC from humid gas streams. *Chem. Mater.*, 2013, **25**, 2591–2596.
- (S11) D. F. Sava, T. J. Garino and T. M. Nenoff, Iodine confinement into metal–organic frameworks (MOFs): Low-temperature sintering glasses to form

novel glass composite material (GCM) alternative waste forms. *Ind. Eng. Chem. Res.*, 2012, **51**, 614–620.

(S12) K. W. Chapman, P. J. Chupas and T. M. Nenoff, Radioactive iodine capture in silver-containing mordenites through nanoscale silver iodide formation. *J. Am. Chem. Soc.*, 2010, **132**, 8897-8899.

(S13) A. P. Katsoulidis, J. He and M. G. Kanatzidis, Functional monolithic polymeric organic framework aerogel as reducing and hosting media for Ag nanoparticles and application in capturing of iodine vapors. *Chem. Mater.*, 2012, **24**, 1937-1943.

(S14) T. Hasell, M. Schmidtman, A. I. Cooper, Molecular doping of organic cages. *J. Am. Chem. Soc.*, 2011, **133**, 14920-14923.

Table S2. Fractional atomic coordinates for the unit cell of **SIOC-COF-7** with AA stacking.

SIOC-COF-7: Space group symmetry P1				
a = 32.35 Å, b=18.36 Å, c= 3.82 Å				
$\alpha = \beta = 90^\circ, \gamma = 122.04^\circ$				
Element	Number	u (Å)	v (Å)	w (Å)
H	1	0.17119	0.097278	0.780994
H	2	0.24511	0.099715	0.810212
H	3	0.32448	0.363944	0.447521
H	4	0.25274	0.367589	0.495969
H	5	0.22994	0.386286	1.047022
H	6	0.24724	0.529947	0.966128
H	7	0.12371	0.431881	0.265095
H	8	0.11126	0.290255	0.307042
H	9	0.0675	0.208816	0.641

H	10	-0.00696	0.088439	0.830777
H	11	0.07014	-0.0101	1.37599
H	12	0.14633	0.115814	1.213048
H	13	0.17178	0.589678	0.400403
H	14	0.30262	0.104146	0.568392
H	15	0.45774	0.358131	0.943725
H	16	0.44829	0.114795	0.608323
H	17	0.51711	0.108517	0.799198
H	18	0.56455	0.32992	1.460329
H	19	0.49552	0.334168	1.295446
H	20	0.49688	0.048895	1.292669
H	21	0.48271	-0.09047	1.340272
H	22	0.63687	0.014657	1.477846
H	23	0.65265	0.157157	1.423467
H	24	0.66275	0.222938	0.91423
H	25	0.74657	0.343971	0.923267
H	26	0.70472	0.478774	1.625515
H	27	0.62368	0.354086	1.658741
H	28	0.35863	0.399998	0.927898
H	29	0.80913	0.487296	1.097979
H	30	0.52702	0.583997	0.991052
H	31	0.5594	0.731537	1.178889
H	32	0.41209	0.672667	1.344499
H	33	0.37971	0.525137	1.155497
H	34	0.32747	0.759251	0.888907
H	35	0.36716	0.914953	0.862919
H	36	0.23866	0.885718	0.365394
H	37	0.19891	0.729755	0.390576

H	38	0.88354	0.590902	1.222915
H	39	0.96023	0.728963	1.185457
H	40	0.88833	0.857102	1.556047
H	41	0.8113	0.71872	1.594009
H	42	0.38632	1.047457	0.940945
H	43	0.58097	0.854945	1.442391
H	44	0.94466	0.953289	1.130606
C	1	0.16817	-2.67548	-0.30509
C	2	0.11578	-2.82853	-0.12442
C	3	0.20467	-2.7644	-0.31129
C	4	0.20489	-2.84021	-0.26139
C	5	0.2474	-2.84074	-0.26959
C	6	0.29353	-2.76591	-0.3503
C	7	0.29133	-2.6945	-0.46042
C	8	0.24936	-2.69294	-0.42841
C	9	0.20629	-2.60437	-0.12825
C	10	0.21593	-2.52208	-0.17636
C	11	0.18676	-2.50553	-0.39135
C	12	0.1473	-2.57682	-0.55524
C	13	0.13891	-2.65911	-0.52214
C	14	0.07063	-2.83747	-0.19963
C	15	0.02663	-2.90801	-0.08751
C	16	0.02411	-2.97478	0.106545
C	17	0.06893	-2.96296	0.2061
C	18	0.11307	-2.89152	0.101413
C	19	0.19772	-2.41914	-0.44783
C	20	0.33848	-2.76281	-0.30213
C	21	0.33725	-2.84032	-0.33962

C	22	0.37401	-2.85207	-0.23745
C	23	0.41982	-2.7771	-0.14135
C	24	0.42233	-2.69809	-0.13083
C	25	0.38351	-2.6884	-0.18469
C	26	0.46283	-2.77778	-0.0531
C	27	0.47233	-2.83914	-0.19159
C	28	0.51222	-2.84187	-0.08812
C	29	0.54686	-2.78415	0.153764
C	30	0.54032	-2.71805	0.268025
C	31	0.49981	-2.71562	0.172995
C	32	0.635	-2.72189	0.275503
C	33	0.57703	-2.88089	0.319111
C	34	0.52957	-2.9549	0.314947
C	35	0.52088	-3.03682	0.354303
C	36	0.5586	-3.05182	0.402702
C	37	0.60556	-2.97864	0.429773
C	38	0.61462	-2.896	0.39221
C	39	0.67198	-2.7214	0.07981
C	40	0.71976	-2.65173	0.083941
C	41	0.73345	-2.57662	0.270856
C	42	0.69648	-2.57691	0.463777
C	43	0.64893	-2.64756	0.471642
C	44	0.39072	-2.60479	-0.10806
C	45	0.78349	-2.50476	0.258028
C	46	0.26009	-2.26782	-0.35583
C	47	0.45102	-2.45683	0.055118
C	48	0.84079	-2.35633	0.406967
C	49	0.5014	-2.39694	0.070346

C	50	0.51972	-2.31346	0.179581
C	51	0.48819	-2.28634	0.280337
C	52	0.43777	-2.34657	0.269456
C	53	0.41943	-2.43012	0.160049
C	54	0.30762	-2.21336	-0.22851
C	55	0.33011	-2.12502	-0.24328
C	56	0.30571	-2.08745	-0.3864
C	57	0.25851	-2.1419	-0.51919
C	58	0.23601	-2.23026	-0.50428
C	59	0.88388	-2.35111	0.299017
C	60	0.92759	-2.27277	0.279148
C	61	0.93038	-2.19589	0.363211
C	62	0.8877	-2.20132	0.482317
C	63	0.84407	-2.27972	0.504608
C	64	0.36375	-1.93923	-0.22995
C	65	0.54935	-2.13792	0.423961
C	66	0.97704	-2.04902	0.197673
N	1	0.16189	-2.75852	-0.25912
N	2	0.58594	-2.79524	0.265505
N	3	0.23881	-2.35659	-0.3285
N	4	0.43469	-2.54003	-0.06088
N	5	0.79528	-2.43388	0.416463
N	6	0.32607	-1.99876	-0.39715
N	7	0.50504	-2.20138	0.373858
N	8	0.97454	-2.11716	0.3189

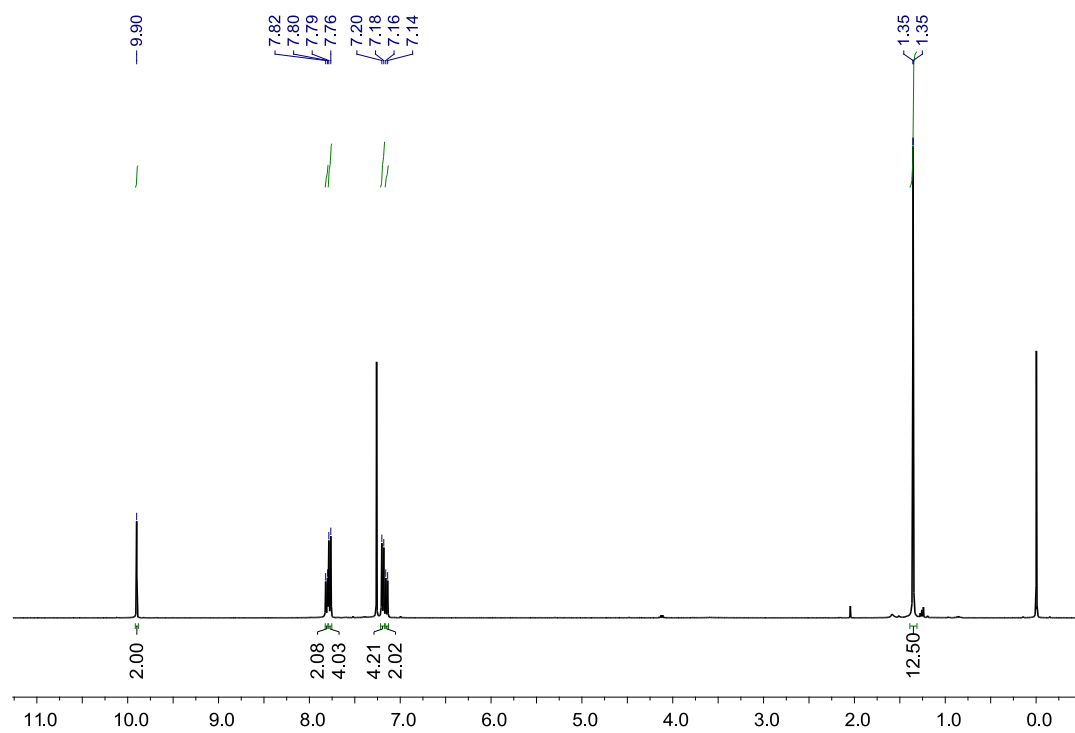


Fig. S9 ^1H NMR (400 MHz, CDCl_3) spectrum of compound **6**.

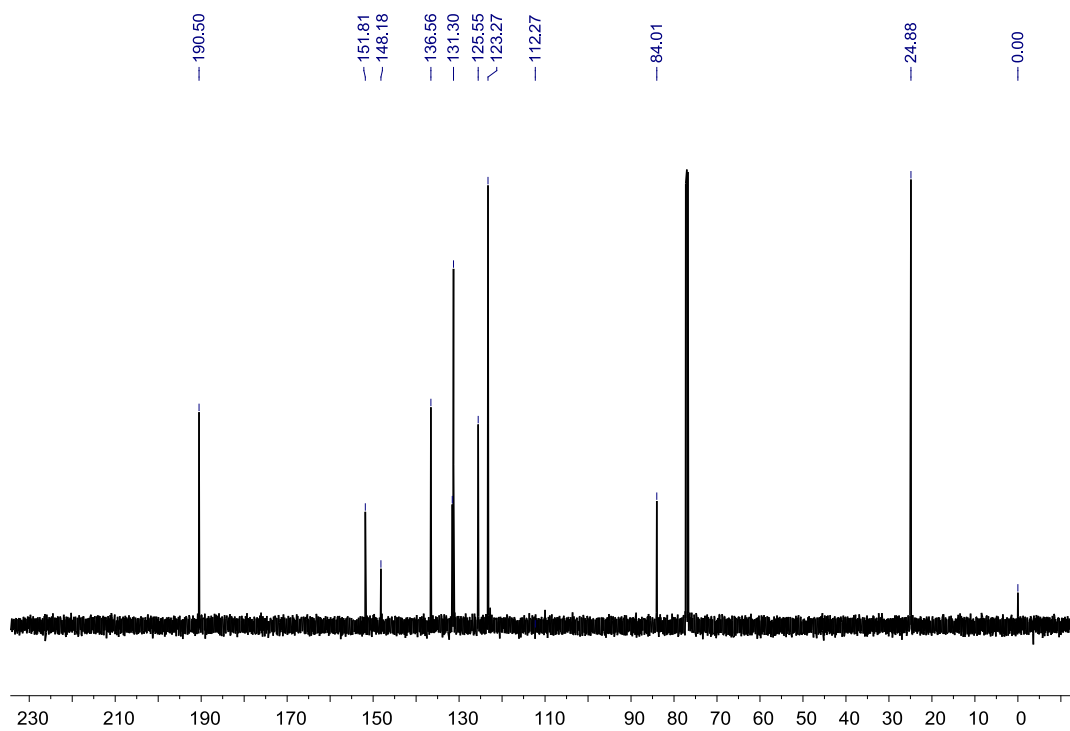


Fig. S10 ^{13}C NMR (125 MHz, CDCl_3) spectrum of compound **6**.

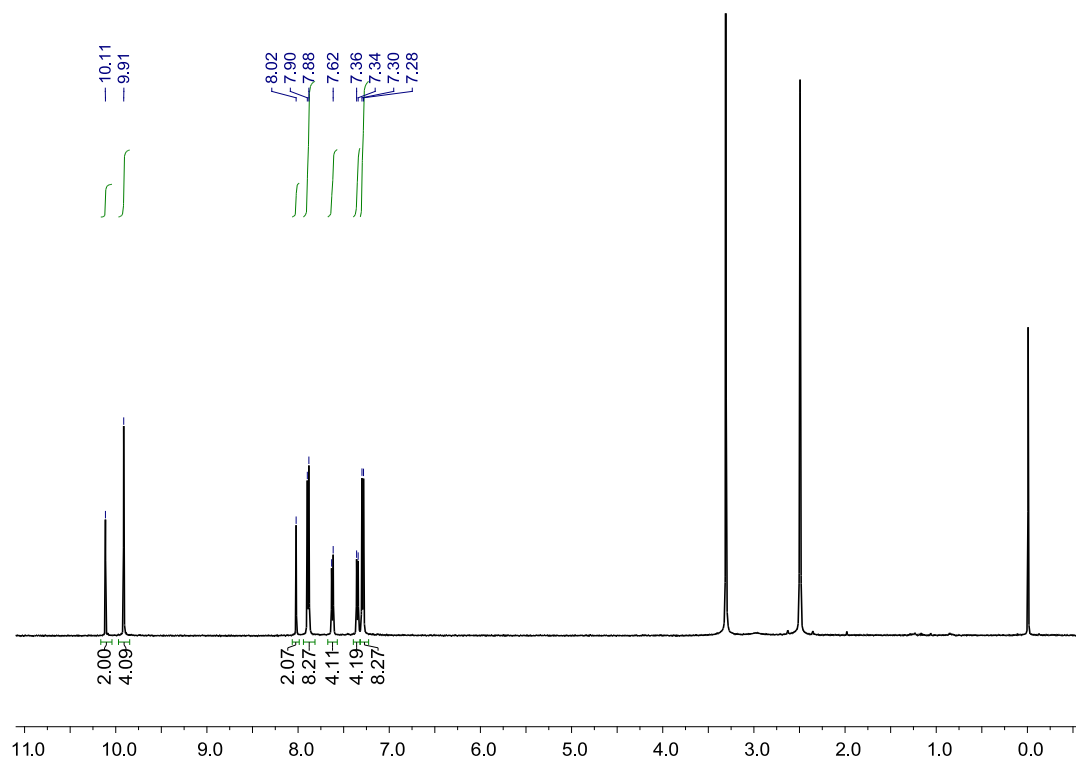


Fig. S11 ^1H NMR (500 MHz, $\text{DMSO-}d_6$) spectrum of **BFATD**.

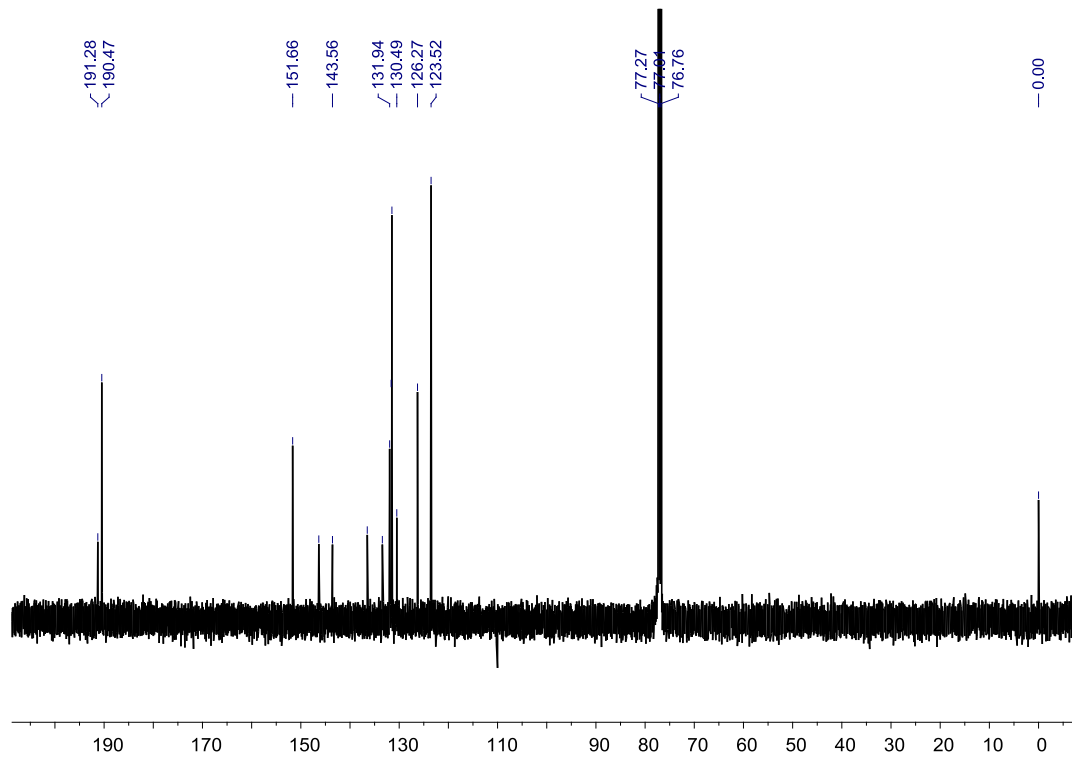


Fig. S12 ^{13}C NMR (125 MHz, CDCl_3) spectrum of compound **BFATD**.